International Journal of Innovative
Computing, Information and Control
Volume **15**, Number **5**, October **2019**

 ISSN 1349-4198
pp. **1947–1965**

TRAIN OPERATION STRATEGY OPTIMIZATION BASED ON IMPROVED GENETIC ALGORITHM

Kaiwei Liu[1], Xingcheng Wang[1], Longda Wang[1] and Gang Liu[2]

[1]School of Marine Electrical Engineering
Dalian Maritime University
No. 1, Linghai Road, Dalian 116026, P. R. China
dmuwxc@dlmu.edu.cn

[2]School of Mechanical Engineering
Inner Mongolia University for the Nationalities
No. 536, Huolinhe Street, Tongliao 028000, P. R. China
liugang530242@163.com

Received December 2018; revised April 2019

Abstract. *The multi-objective optimization problem in train operation is a nonlinear control problem which is affected by many kinds of constraints and parameters. There are more than one or infinite Pareto solutions in the optimal solution set, so it is very difficult to obtain an accurate train control sequence. So, taking the energy consumption, punctuality and comfort as the optimization objectives, and combining the dynamic equation and constraint equation of urban rail train, the multi-objective optimization model of train operation process is established in this paper. At the same time, an adaptive Genetic Algorithm (GA) based on Directional Mutation (DM) and Gene Modification (GM) is proposed to solve the optimization model. In addition, the fusion distance is used to judge the existence of individual aggregation phenomenon at the late stage of iteration for GA, thereby inhibiting the local convergence. Both MATLAB simulation results and HIL (Hardware-in-the-Loop) simulation results show that the improved GA can quickly obtain an accurate control sequence of train operation, which has great reference value for the actual train operation control.*

Keywords: Train operation optimization, Genetic algorithm, Directional mutation, Gene modification, Fusion distance

1. **Introduction.** The train operation system is a typical complex and multi-objective nonlinear control system. In the operation process, the train is affected by vehicle condition, line condition, traction power supply system and various constraints, has a mass of uncertainty and has multiple optimization objectives that conflict with each other. Therefore, it is very difficult to find a control sequence that can simultaneously take account of multiple optimization objectives such as safety, punctuality, energy saving and comfort among numerous train control sequences. However, traditional control methods often have higher requirements on the accuracy of the mathematical model, so it is difficult for traditional control methods to achieve ideal results in such a complex process. With the development of intelligent optimization theory, the intelligent optimization algorithms show irreplaceable advantages in solving multi-objective optimization problems [1,2]. As a kind of intelligent optimization algorithm, GA has been widely used in train automatic control [3,4]. Due to the disadvantages of GA, such as large amount of calculation and long solving time, the scholars in relevant field have improved it. In [5], a GA of fuzzy

DOI: 10.24507/ijicic.15.05.1947

parameter based on accurate simulation of train motion is proposed for online optimization of Automatic Train Operation (ATO). In [6], several performance indexes of the train automatic running speed curve model are designed, and the ATO velocity curve is optimized by adaptive GA. In [7], an improved multi-objective GA with variable chromosome length is proposed to optimize and solve the train operation simulation model. In [8], an improved multi-objective GA is proposed. Penalty function is added to fitness objective function and the model is optimized from five aspects: speed (safety), parking accuracy, punctuality, energy consumption and comfort. In [9], the Multi-Population Genetic Algorithm (MPGA) is used to solve the energy-saving optimization model of metro train, which considers both travel time and driving strategy. However, in the above literature, the evolutionary direction of single chromosome in GA is random, so the evolutionary direction may be good or bad. The chromosomes that evolve in the negative direction are not only unhelpful in finding the optimal solution, but also increase the computation time and slow down the convergence speed of GA.

To solve the above problems and improve the convergence speed of GA, an adaptive GA based on DM and GM is proposed to solve the train multi-objective optimization model in this paper. DM is derived from the gradient function. Since the gradient function changes the most in a certain direction, the method based on gradient can always converge at a faster speed. If the gradient information is introduced into GA to determine the mutation direction while ensuring the global optimality of GA, the convergence speed of GA will be accelerated. As there are many constraints in train operation process, the search speed for individuals who satisfy all constraints is slow in the more complex interval only through random crossover and mutation. Therefore, according to the traditional experience, relevant genes are modified to generate new genes within a reasonable range to meet all constraints. DM and GM can guide the mutation operation to the optimal direction with greater probability, thus improving efficiency of GA. In addition, GA is prone to local convergence at the end stage of iteration, and there are a large number of individuals in the smaller neighborhood of the optimal individual. Therefore, fusion distance which integrates Mahalanobis distance and Euclidean distance is used to judge the existence of individual aggregation phenomenon in this paper, which is more conducive to suppress the local convergence.

On the basis of the traditional GA, the classical operations of selection and crossover are preserved, and the mutation operation is further improved in this paper. Traditional mutation is a kind of random mutation operation, but in this paper, DM and GM are performed to the relevant genes according to the type of penalty function, so as to avoid blind random mutation and greatly improve the efficiency of the algorithm. In addition, in the late iteration of the GA, the fusion distance measurement method can be used to find the clustered individuals more quickly and accurately, so as to carry out corresponding operations on these individuals. The simulation results show that the improved GA has better performance in train operation optimization.

2. Mathematical Model of Train Operation Process.

2.1. Train dynamical model.

The dynamic equation of train operation is as follows [10]:

$$\begin{cases} \dfrac{dt}{ds} = \dfrac{1}{v} \\ Mv\dfrac{dv}{ds} = f(u,v) - w(v,s) - b(u,v) \end{cases} \tag{1}$$

where t represents the actual running time of the train; s denotes the actual position of the train; v is the actual speed of the train; M is the quality of the train; $f(u,v)$ and $b(u,v)$ are tractive force and braking force of the train (f and b are determined by the train's current speed v and control sequence u); $w(v,s)$ is the additional resistance of the train, which is determined by the current speed v and actual position s of the train; u represents the train control sequence, which is represented by five control modes $\{1, 0.5, 0, -0.5, -1\}$. These five control modes are a typical control scheme, which are divided according to the principle that the train is accelerated or decelerated by its own internal power and are related to the state of traction motor in the process of train operation [11]. 1 represents the maximum traction; -1 denotes the maximum braking; 0 represents coasting operation, where the train exerts no traction or braking force; -0.5 and 0.5 respectively denote partial braking and partial traction, where the train is in a constant speed state.

2.2. **Constraints on the train operation.** In order to ensure the safe and stable operation of the train, many constraints such as the line conditions should be considered.

2.2.1. *Boundary constraint.* The speed and distance of the train in the initial state are 0, and the final speed at the terminal station is also 0.

$$\begin{cases} v_{initial} = 0, \ v_{final} = 0 \\ s_{initial} = 0, \ s_{final} = D \end{cases} \tag{2}$$

where D stands for the total distance between two stations.

2.2.2. *Position variable constraint.* The positions corresponding to the working condition conversion should keep increasing order.

$$0 < S_1 < S_2 < \cdots < S_j < D \tag{3}$$

where S_j stands for the position corresponding to each working condition conversion.

2.2.3. *The speed limit constraint.* In order to ensure the safety of train operation and prevent accidents such as derailment, the speed limit is needed.

$$V_x = \begin{cases} 0 \le v \le V_x \\ V_{x1} \, (S_0 \le S < S_1) \\ V_{x2} \, (S_1 \le S < S_2) \\ V_{x3} \, (S_2 \le S < S_3) \\ \cdots \\ V_{xz} \, (S_{z-1} \le S \le S_z) \end{cases} \tag{4}$$

where V_x is the maximum running speed allowed by the subinterval.

2.3. **Multi-objective optimization model.** The urban rail train system is a complex nonlinear system, which has many input and output variables. So, taking the energy consumption, punctuality and comfort as the optimization objectives, and combining the dynamic equation and constraint equation of urban rail train, the multi-objective

optimization model of train operation process is established in this paper.

$$\begin{cases} K_E = \sum_{i=1}^{n} (Ma_i - R_i)(s_i - s_{i-1}) \\ K_A = \sum_{i=2}^{n} |a_i - a_{i-1}| \\ K_T = \left| \sum_{i=1}^{n} \left[\left(\sqrt{2a_i (s_i - s_{i-1}) + v_{i-1}^2} - v_{i-1} \right) \Big/ a_i \right] - T \right| \\ F(u) = (K_E(u), K_A(u), K_T(u)) \\ \min \{F(u)\} \end{cases} \tag{5}$$

where K_E is the energy consumed by the traction force during the train operation; K_A represents comfort level of passengers, which is expressed by the sum of the absolute value of the difference in acceleration of the adjacent working conditions; K_T is the absolute value of the difference between the actual running time and the prescribed running time; $F(u)$ is the multi-objective optimization model.

Compared with the multi-objective optimization problem, the single objective optimization problem is easier to be solved. It is a practical and effective way to transform the multi-objective optimization problem into single-objective optimization problem. In this paper, the weighted-sum approach is used to solve multi-objective optimization problem [2].

$$\begin{cases} f = \sum_{i=1}^{3} \omega_i f_i^g \\ f_i^g = \dfrac{f_i - \min f_i}{\max f_i - \min f_i} \end{cases} \tag{6}$$

where ω_i represents the weight coefficient ($\sum_{i=1}^{3} \omega_i = 1$), which reflects the relative importance of the ith optimization objective; f_i^g denotes the normalized value of each optimization target, which eliminates the negative influence caused by the dimensional difference for the ith optimization goal.

3. Train Operation Optimization Based on Improved GA.

GA belongs to an important branch of evolutionary algorithm, which is an algorithm that uses the natural selection of biological world for reference and simulates the mechanism of biological evolution. GA uses random rules to search in the global scope. For complex line conditions, the search speed for feasible solution is slow. Therefore, an adaptive GA based on DM and GM is used to accelerate the search for feasible solution in this paper. Since GA is prone to local convergence in the late stage of iteration, the fusion distance is proposed to detect the existence of individual aggregation phenomenon, thereby inhibiting the local convergence.

3.1. Gene coding design.

Coding is to transform the solution space of the problem into the searching space that the intelligent algorithm can handle. Real number coding is very intuitive and can save coding and decoding operations, so it is adopted in this paper. The number of variables of the solution should be determined before coding. If there are too many variables to be solved, the search space will be too large. At this time, the algorithm will take a long time and the optimal solution will not be easily found. Therefore, the following coding mechanism is used to solve the above problem.

(1) There is no static speed limit falling interval and the corresponding diagram of train operation mode is shown in Figure 1.

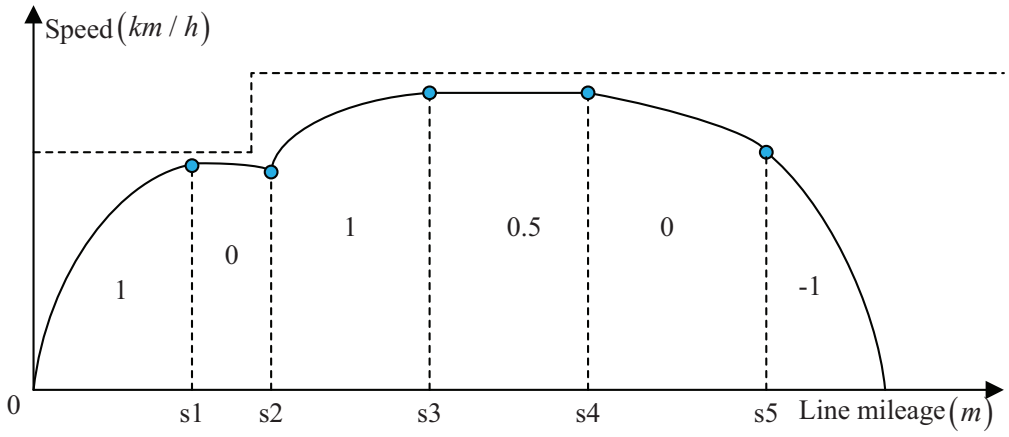

FIGURE 1. Diagram of train operation mode

In Figure 1, the dotted line represents the speed limit condition. Trains leave the station with maximum traction, so the solution can be set as shown below, which omits the maximum traction mode:

$$X = (0, 1, 0.5, 0, -1, s1, s2, s3, s4, s5) \tag{7}$$

The first part of solution X is the working condition (control modes), and the second part of solution X represents the position corresponding to the working condition conversion.

(2) There is the static speed limit falling interval, and the corresponding diagram of train operation mode is shown in Figure 2.

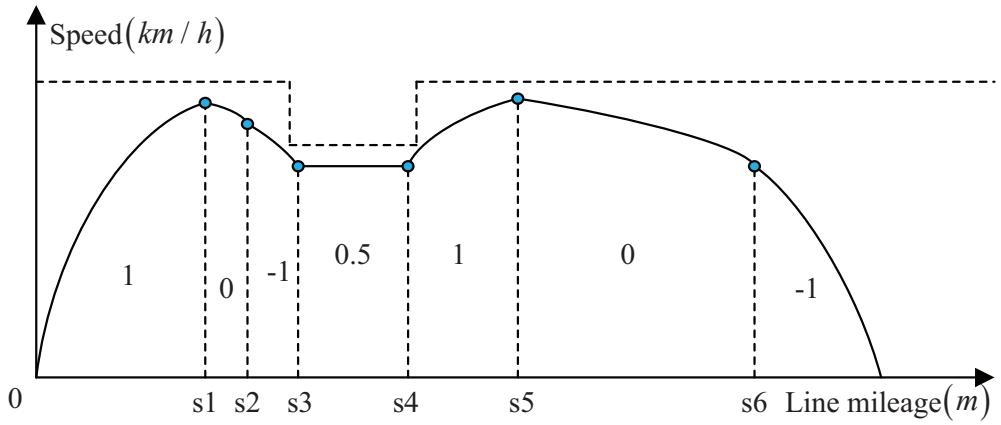

FIGURE 2. Diagram of train operation mode

The solution is set as shown below:

$$X = (0, -1, 0.5, 1, 0, -1, s1, s2, s3, s4, s5, s6) \tag{8}$$

(3) There is the static speed limit falling and rising interval, and the corresponding diagram of train operation mode is shown in Figure 3.

The solution is set as shown below:

$$X = (0, 1, 0, -1, 0.5, 1, 0, -1, s1, s2, s3, s4, s5, s6, s7, s8) \tag{9}$$

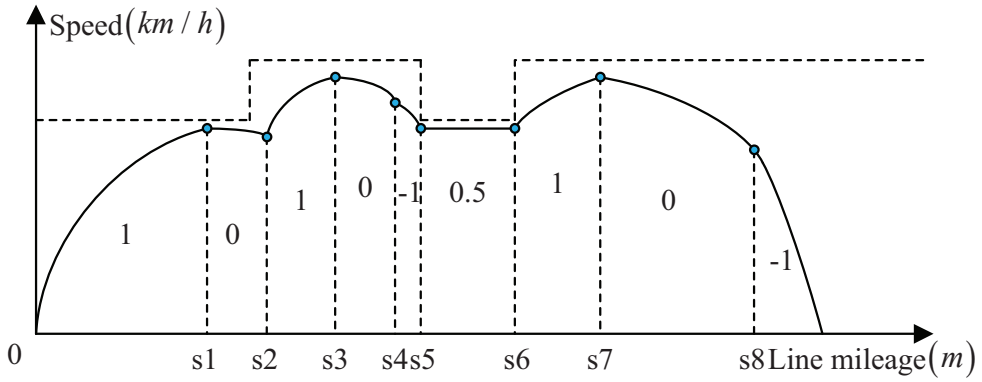

FIGURE 3. Diagram of train operation mode

Any complex speed limit interval can be composed of the above three basic speed limit intervals, and the coding mechanisms of three basic speed intervals are also applicable to any complex speed limit interval. Based on previous research results, the following conclusion can be obtained. When the train keeps coasting condition or constant speed running condition, the energy consumed by train is the least. The coding mechanism in this paper fully follows the energy minimum principle, which can reduce the energy consumed by urban rail train to the greatest extent.

3.2. **GA based on DM and GM.**

3.2.1. *DM.* Since the gradient represents the direction in which the function changes most, the method based on gradient can always converge at a faster speed. In this paper, the information that is similar to gradient is introduced into GA to determine the direction of mutation, which can improve the convergence speed and efficiency of the algorithm.

The direction of mutation is determined by the vector difference of two individuals. For the minimum optimization problem $\min\{f(X)\}$, $X = [x_1, x_2, \ldots, x_n]^T$, take two individuals X_k, X_{k+1}, and $y_k = f(X_k)$, $y_{k+1} = f(X_{k+1})$. Define the vector $d(X_{k+1}, X_k) = \operatorname{sgn}(X_{k+1} - X_k) = \operatorname{sgn}\left([x_{k+1,1} - x_{k,1}, x_{k+1,2} - x_{k,2}, \ldots, x_{k+1,n} - x_{k,n}]^T\right)$. When $y_{k+1} \leq y_k$, the vector $d(X_{k+1}, X_k)$ is the evolutionary direction of $f(x)$ from X_k to X_{k+1}. When $y_{k+1} \geq y_k$, the vector $d(X_{k+1}, X_k)$ is the degenerate direction of $f(x)$ from X_k to X_{k+1}.

3.2.2. *Penalty function.* Two constraint conditions of speed limit and parking error in the process of train operation are added to the objective function in the form of penalty function. Generally, there are two methods to deal with the over-limit. The experimental results show that the second method is more effective; therefore, the second method is used to construct the penalty function.

(1) Add the sum of squares of all the over-limit sizes to the penalty term.

$$P = a\sum_{i}^{n}\left(\max\left[0, (v_i - v_{i\max})\right]\right)^2 + b(\max\left[0, (|s_p - s'| - 0.2)\right])^2 = P_1 + P_2 \tag{10}$$

where s_p represents the actual running distance of the train; s' is the distance between two stations; the parameters a, b are the weighting coefficients of the penalty function; the parking error is within the range of ± 20 cm.

(2) Add the square of the maximum over-limit size to the penalty term.

$$P = a\max_{i}^{n}\Delta v_i^2 + b(\max\left[0, (|s_p - s'| - 0.2)\right])^2 = P_1 + P_2 \tag{11}$$

where $\Delta v_i^2 = (\max[0, (v_i - v_{i\max})])^2$.

3.2.3. *GM.* Because there are many constraints on train operation control, the search speed for the feasible solution obtained only by random crossover and mutation is slow for complex lines. Therefore, by using the traditional experience for reference, the related genes will be modified according to the type of penalty term for the individuals whose penalty function value is not zero.

(1) The penalty term P_1 of speed is not zero, and the diagrams of train operation mode are as shown in Figures 4 and 5.

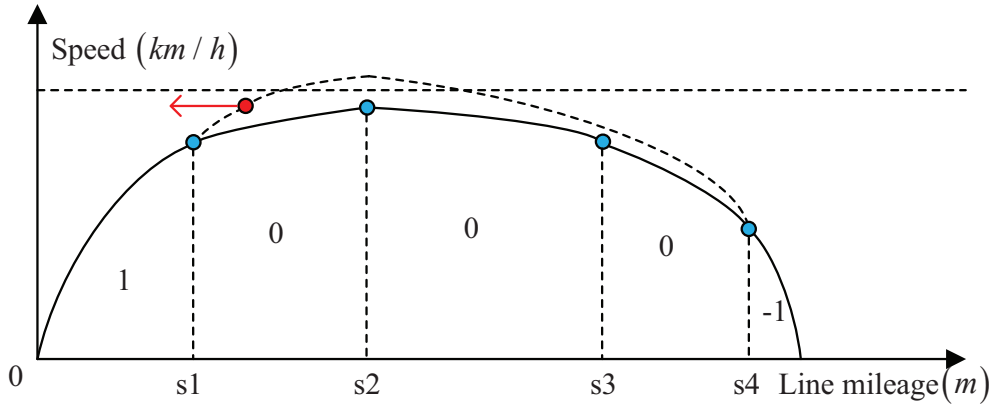

FIGURE 4. Diagram of train operation mode (overspeed in coasting condition)

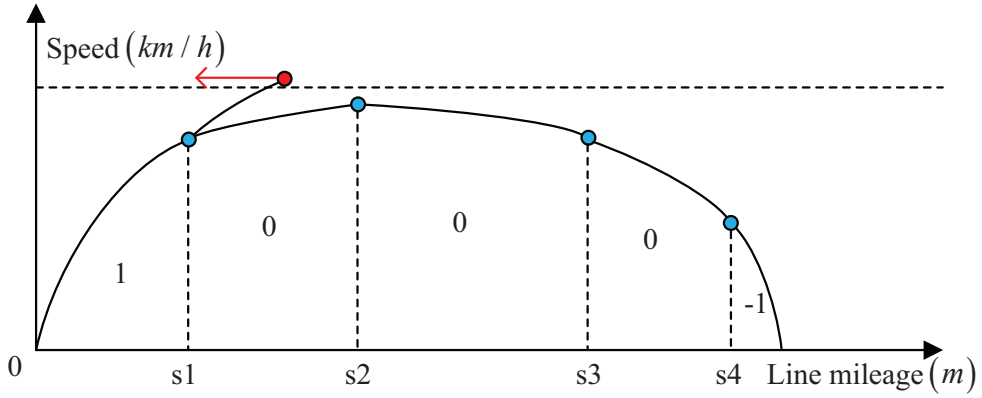

FIGURE 5. Diagram of train operation mode (overspeed in traction condition)

As shown in Figures 4 and 5, if the train runs according to the original control strategy, it will show overspeed. At this time, GM should be made to move the working condition point with the arrow to the left. The working condition point with the arrow in Figures 4 and 5 is set as s_1', and the formula for GM is as follows:

$$s_1 = s_1' - \alpha \cdot rand \tag{12}$$

where α is the coefficient of GM, which determines the degree of GM. *rand* represents random number between 0 and 1.

(2) The penalty term P_2 of parking error is not zero, and the diagrams of train operation mode are as shown in Figures 6 and 7.

s_p represents the actual running distance of the train; s' denotes the distance between the two stations. In Figure 6, the actual running distance s_p is larger than s'. At this

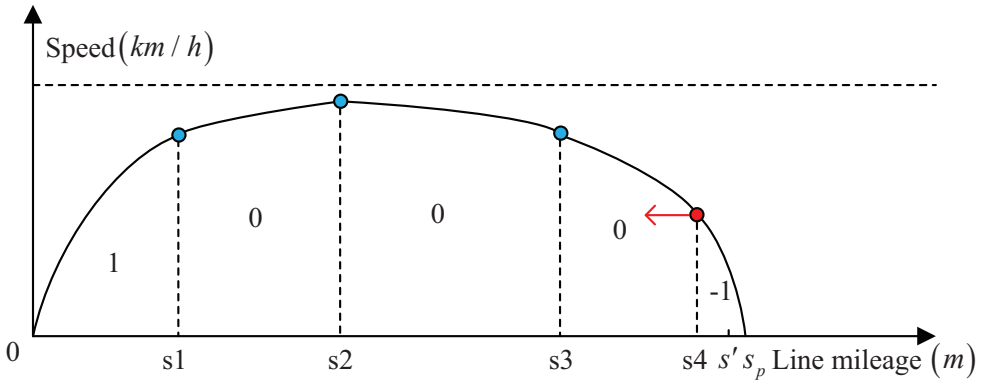

FIGURE 6. Diagram of train operation mode (cross line)

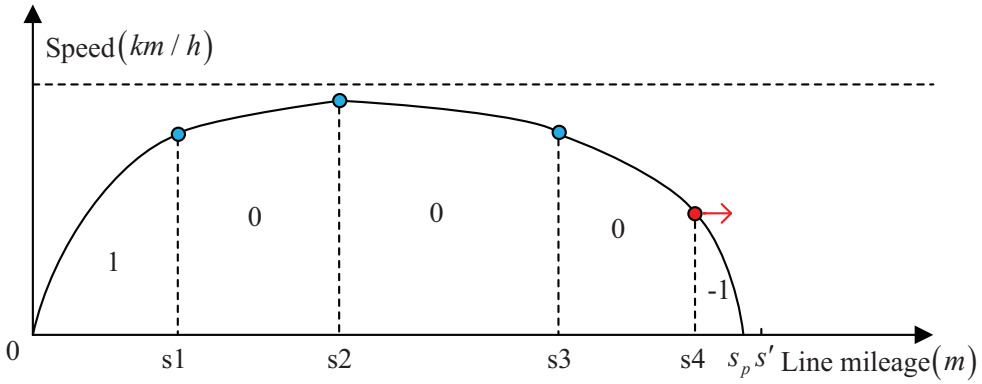

FIGURE 7. Diagram of train operation mode (not cross line)

time, the barking point with the arrow should move to the left. In Figure 7, the actual running distance s_p is less than s'. At this time, the barking point with the arrow should move to the right. The braking point after GM is set as s'_4, and the formula for GM is as follows:

$$s'_4 = s_4 \mp \beta \cdot rand \tag{13}$$

where β is the coefficient of GM, which determines the degree of GM.

3.2.4. *Construction of fitness function.* Fitness function is the only basis of natural evolutionary selection. The objective function needs to be converted into fitness function according to a certain conversion rule. Because the optimization model of train operation process has multiple constraints, the penalty function can be added to the fitness function. In this way, the constrained problem can be transformed into the unconstrained problem. If the value of the penalty function is 0, which indicates that the individual satisfies the constraint conditions, the DM will be carried. If the value of the penalty function is not 0, which indicates that the individual does not satisfy the constraint conditions, the GM will be carried.

$$Fit(X) = \frac{1}{f(X) + P(X)} \tag{14}$$

where $f(X)$ is objective function; $P(X)$ is penalty function.

3.2.5. *Adaptive crossover and mutation probability.* In the early stage of evolution, individuals in the population are relatively scattered and have large adaptability differences.

At this time, GA should search in a wide range, which can not only improve the adaptability of individuals as soon as possible but also avoid the premature convergence. In the later stage of evolution, individual differences in the population become smaller, and individuals are relatively concentrated. At this point, the algorithm conducts local search. Too high crossover and mutation probability may destroy excellent individual genes, while too small probability makes it easy for GA to fall into local optimum. Therefore, the dynamic adjustment of crossover and mutation probability is the key to the reasonable evolution for GA, and the individual can dynamically adjust the corresponding probability value according to its fitness function value [6]. Individuals with higher function fitness values generally have better genes, and low crossover and mutation probability should be adopted for such individuals. For the individuals with low fitness values, high crossover and mutation probability should be adopted.

$$Pc = \begin{cases} Pc_2 & F' \le \bar{F} - \eta \\ \dfrac{Pc_1 + Pc_2}{2} & \bar{F} - \eta < F' \le \bar{F} \\ Pc_1 + \dfrac{Pc_2 - Pc_1}{2} \cdot \dfrac{F_{\max} - F'}{\eta} & \bar{F} < F' \le F_{\max} \end{cases} \tag{15}$$

$$Pm = \begin{cases} Pm_2 & F \le \bar{F} - \eta \\ \dfrac{Pm_1 + Pm_2}{2} & \bar{F} - \eta < F \le \bar{F} \\ Pm_1 + \dfrac{Pm_2 - Pm_1}{2} \cdot \dfrac{F_{\max} - F}{\eta} & \bar{F} < F \le F_{\max} \end{cases} \tag{16}$$

where Pc is the crossover probability; Pm is the mutation probability; Pc_1 and Pc_2 represent the minimum and maximum crossover probability; Pm_1 and Pm_2 represent the minimum and maximum mutation probability; F' represents the larger fitness value between two chromosomes that need to be crossed; $\bar{F}$ represents the average fitness value of the current population; $F_{\max}$ is the maximum fitness value in the current population; η is the difference between the fitness value of the optimal individual and the average fitness value in the current population; F is the fitness value of the current individual.

The new adaptive probability formula enables the chromosomes to timely adjust the crossover and mutation probability according to their fitness function values. This new improved method can obviously improve the convergence rate of GA.

3.3. **Improvement strategy of GA based on fusion distance.** The GA is prone to local convergence at the end stage of iteration, and there is a large number of individuals in the smaller neighborhood of the optimal individual. At this time, some of these individuals need to be replaced before the next iteration to prevent them from confining the entire population to a local area. However, using Euclidean distance to judge the existence of local convergence phenomenon has many shortcomings. Euclidean distance does not take account of the distribution of individuals and the correlation among variables, and it measures the linear distance among individuals. Mahalanobis distance which takes account of the correlation among variables is a covariance distance of data. Therefore, the fusion distance is proposed in this paper, which integrates Mahalanobis distance and Euclidean distance [12]. The new measure method takes account of both the independence of variables and the correlation among variables, and improves the precision of distance measurement. The improved fusion distance can be used to effectively judge whether individual aggregation phenomenon occurs.

3.3.1. *The definition of Euclidean distance.* Minkowski distance is a distance formula defined by Minkowski, and Euclidean distance is a special case of Minkowski distance.

$$ED = \left[\sum_{n=1}^{k} |x_{ni} - x_{nj}|^2\right]^{1/2} \tag{17}$$

where x_i and x_j represent two different vectors; n is the dimension of the vector x.

3.3.2. *The definition of Mahalanobis distance.* Mahalanobis distance is a distance defined by Mahalanobis, a famous Indian statistician. Mahalanobis distance which takes account of the correlation among variables is a covariance distance of data. The Mahalanobis distance formula between the individual X and the basic spatial set Y is as follows:

$$MD(X,Y) = \sqrt{\left(X - \overline{Y}\right)' \Sigma^{-1} \left(X - \overline{Y}\right)} = \sqrt{\left(X - \overline{Y}\right)' \Sigma_Y^{-1} \left(X - \overline{Y}\right)} \tag{18}$$

$$\Sigma_Y = \begin{bmatrix} Cov(Y_1, Y_1) & Cov(Y_1, Y_2) & \cdots & Cov(Y_1, Y_j) \\ Cov(Y_2, Y_1) & Cov(Y_2, Y_2) & \cdots & Cov(Y_2, Y_j) \\ \vdots & \vdots & \ddots & \vdots \\ Cov(Y_j, Y_1) & Cov(Y_j, Y_2) & \cdots & Cov(Y_j, Y_j) \end{bmatrix} \tag{19}$$

where Σ is the expectation matrix of the covariance matrix of the basic spatial set Y; $\overline{Y}$ and Σ_Y are the mean and covariance matrices of the basic spatial set Y; Y_i $(i = 1, \ldots, j)$ represents the individual in the basic spatial set Y; j is the number of all individuals in Y. Since Σ is difficult to obtain, Σ_Y can be used to approximately replace Σ.

3.3.3. *The definition of fusion distance.* When the correlation among variables is fuzzy, neither the classical Mahalanobis distance nor Euclidean distance can effectively calculate the distance between the individual X and the basic spatial set Y. The fusion distance takes account of the independence and correlation among variables, which can effectively improve the accuracy of distance calculation. The formula for calculating fusion distance is shown below:

$$\begin{cases} d_{Mix} = \omega \times MD(X,Y) + (1-\omega) \times ED(X,Y) \\ C_Y = \begin{bmatrix} \rho_{Y_1Y_1} & \rho_{Y_1Y_2} & \cdots & \rho_{Y_1Y_n} \\ \rho_{Y_2Y_1} & \rho_{Y_2Y_2} & \cdots & \rho_{Y_2Y_n} \\ \vdots & \vdots & \ddots & \vdots \\ \rho_{Y_nY_1} & \rho_{Y_nY_2} & \cdots & \rho_{Y_nY_n} \end{bmatrix} \\ \omega = \sqrt{1 - |C_Y|} \end{cases} \tag{20}$$

where d_{Mix} is fusion distance; MD is Mahalanobis distance; ED is Euclidean distance; C_Y is the correlation coefficient matrix of the basic spatial set Y; n is the number of individuals in the spatial set Y; Y_i $(i = 1, \ldots, n)$ represents the individual in the basic spatial set Y; ρ is the correlation coefficient. Since Mahalanobis distance takes account of the correlation among variables, it is fused by ω with relevant information, while Euclidean distance is fused by $1 - \omega$.

3.3.4. *The judgment of individual agglomeration phenomenon.* The elite set of GA is the basic spatial set Y mentioned above. The selection of elite set radius is the key to judge the existence of individual agglomeration phenomenon. The radius of elite set is the maximum distance between each individual in elite set and elite set. The Mahalanobis distance between the individual and elite set can be obtained by Formulas (18) and (19). However, the Euclidean distance between the individual and elite set cannot be obtained

by Formula (17). Therefore, the Euclidean distance between the individual and elite set is obtained by the following methods in this paper.

(1) The center position (the average individual in elite set) of elite set can be obtained by the average method.

(2) The Euclidean distance between the individual and elite set will be converted to the Euclidean distance between the individual and the average individual mentioned above.

When the fusion distance between an individual out of elite set and elite set is smaller than the elite set radius, this individual is in the elite set. When the number of individuals like such individual mentioned above is greater than a certain threshold, the individual agglomeration phenomenon occurs. At this point, random crossover and mutation operations can be used to disperse these individuals, which makes the algorithm jump out of the local optimum. The total flowchart of the improved GA is shown in Figure 8.

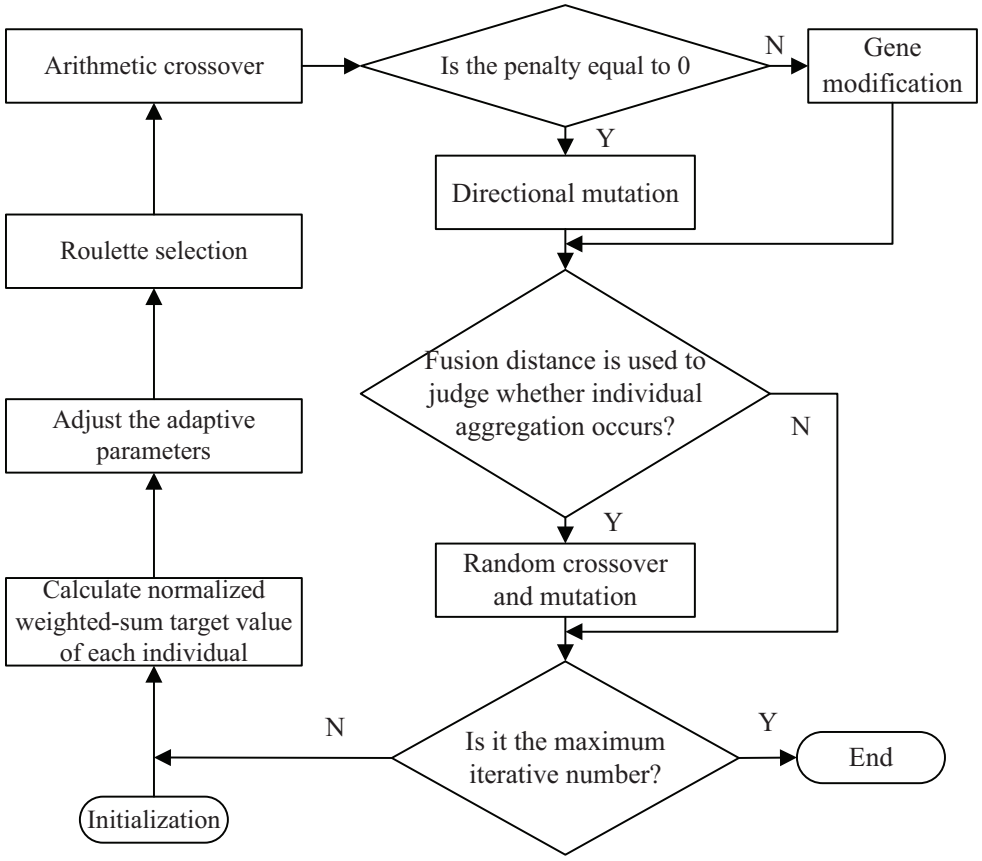

FIGURE 8. The total flowchart of the improved GA

4. **The Experimental Simulation.**

4.1. **Relevant data of train.** In this paper, the train of light rail line 12 in Dalian is selected as the research object. The simulation line is from New Port in Lvshun to Tieshan Town, the length of which is 2.94 km. The basic attributes of the train are shown in Table 1, and the characteristic curves of traction and braking are shown in Figure 9, and train speed limit and slope parameters are shown in Figure 10.

4.2. **Parameter setting.** The following initialization parameters are given in combination with relevant scientific literature, relevant field experience and simulation results of multiple tests: the population size is set to 400; the maximum number of iterations is set

TABLE 1. The basic parameters of train

Parameter name	Parameter characteristics
Train weight (t)	211
Maximum running speed (km/h)	80
Formation plan	2 motor 2 trail
Mean starting acceleration (m/s^2)	$(0 \sim 35$ km/h$) \geq 1.0$
Mean acceleration (m/s^2)	$(0 \sim 80$ km/h$) \geq 0.6$
Mean braking deceleration (m/s^2)	$(80 \sim 0$ km/h$) \geq 1.0$
Rotary mass coefficient (γ)	0.06

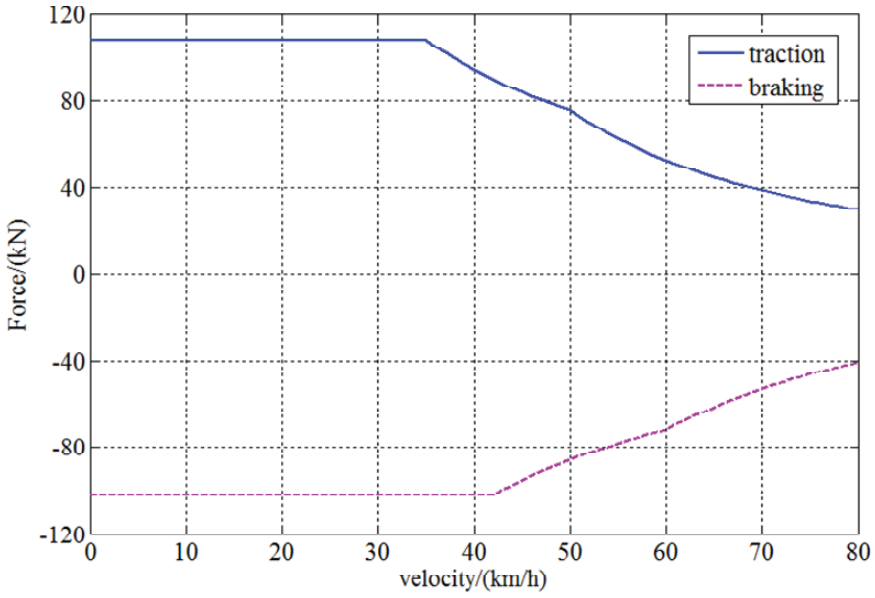

FIGURE 9. The characteristic curves of traction and braking

to 200; $Pc_1 = 20\%$, $Pc_2 = 80\%$, $Pm_1 = 1\%$, $Pm_2 = 10\%$; according to experience, the weight coefficients ω_1, ω_2 and ω_3 for energy consumption, comfort and punctuality are set to 0.5, 0.3 and 0.2 respectively. When the planned running time is 180s, the basic requirements for optimization targets are $K_E \in [80000, 120000]$, $K_A \in [13, 30]$, $K_T \in [0, 2]$.

4.3. **Matlab simulation results and analysis.** In order to verify that the improved GA has better performance, this paper uses the basic GA, the adaptive GA based on DM and GM and the improved GA to solve the train optimization model. The simulation results are shown in Figures 11 to 14 and Table 2. In addition, the three different algorithms are respectively denoted as GA, DG-GA and I-GA. Compared with I-GA, DG-GA has no fusion distance judgment.

It can be seen from Table 2 that the I-GA has a considerable improvement in energy saving, punctuality and comfort level, compared with GA and DG-GA. The total energy consumption of I-GA is 8590 KJ (about 8.0%) lower than that of DG-GA; the total energy consumption of I-GA is 7287 KJ (about 6.8%) lower than that of GA, and the light rail line 12 in Dalian is located in the hilly area, and the hilliness is a typical landform feature in Dalian. In such a terrain, the train needs to accelerate by using the long downhill section and decelerate by using the long uphill section to save energy consumption, and the simple train control sequence can also avoid turbulence. It can be seen from Figure

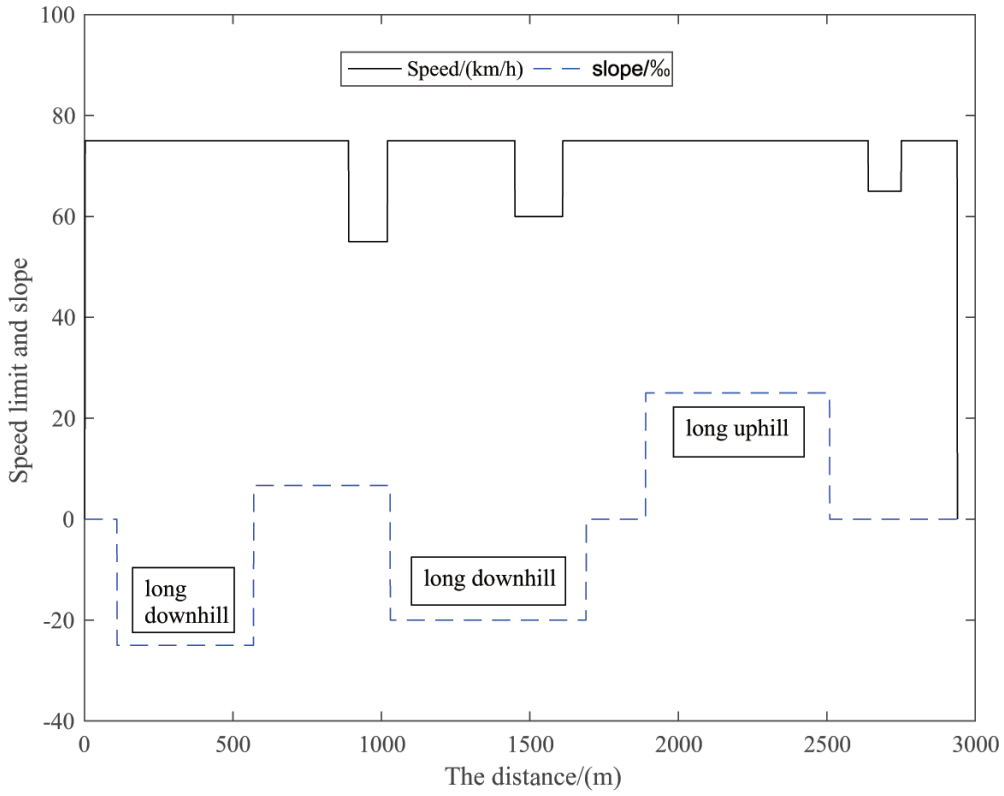

FIGURE 10. The schematic of train speed limit and ramp parameters

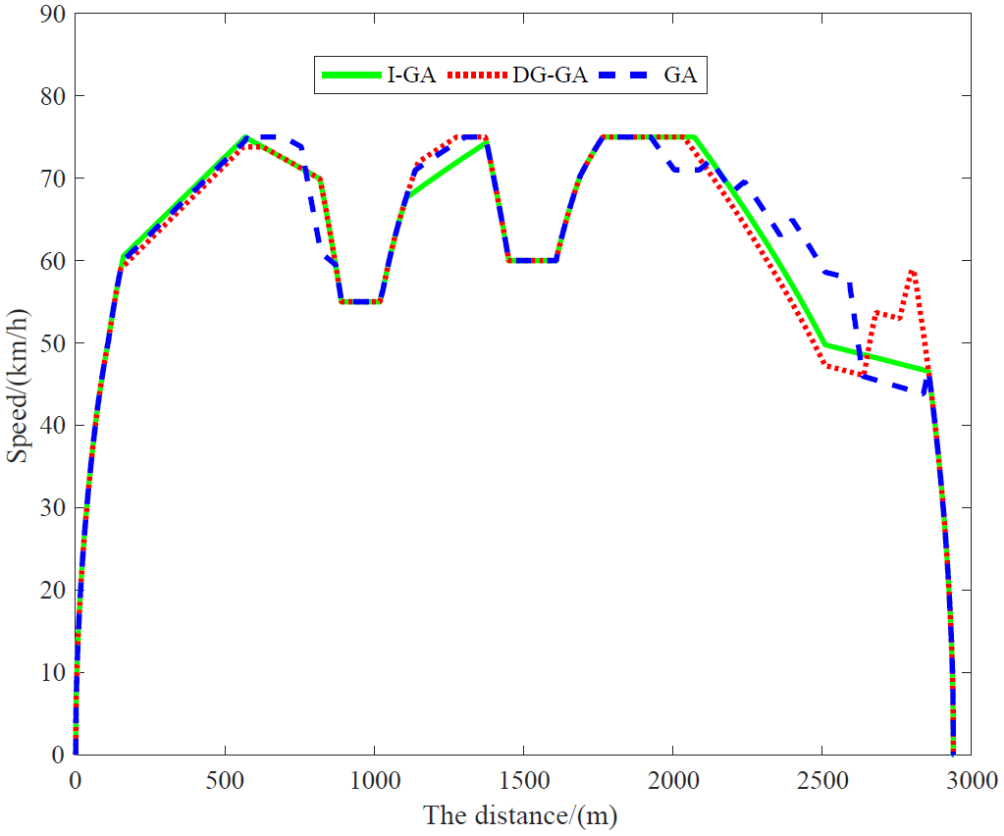

FIGURE 11. The speed distance graph of optimal results

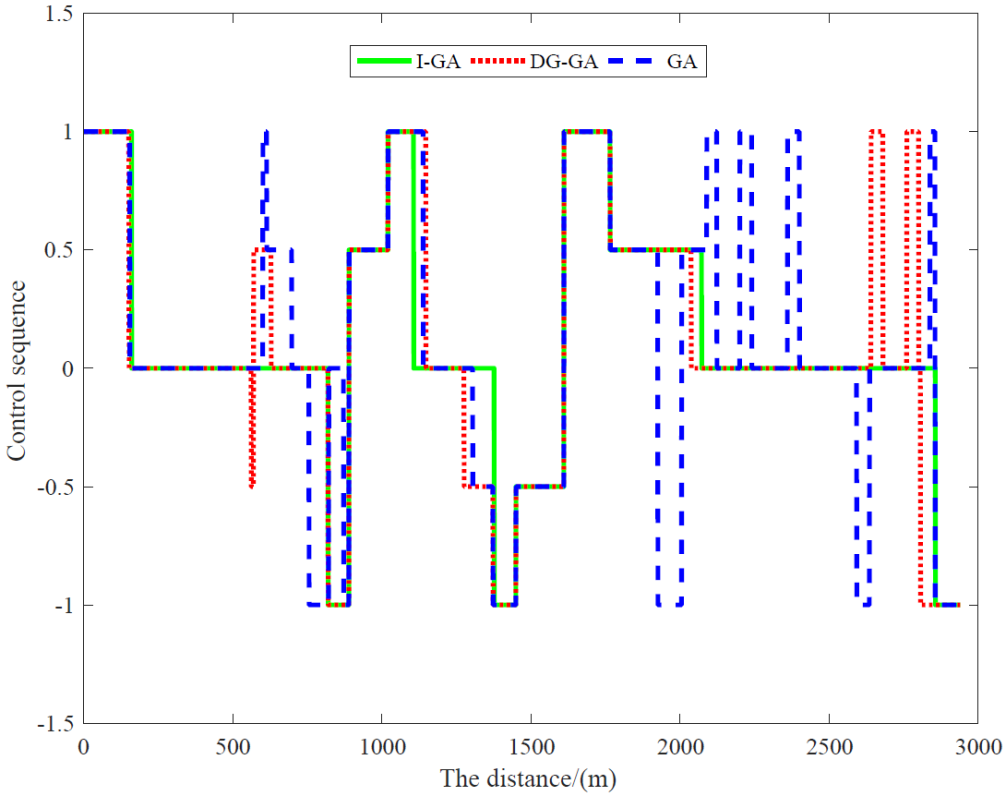

FIGURE 12. Train operation control sequence

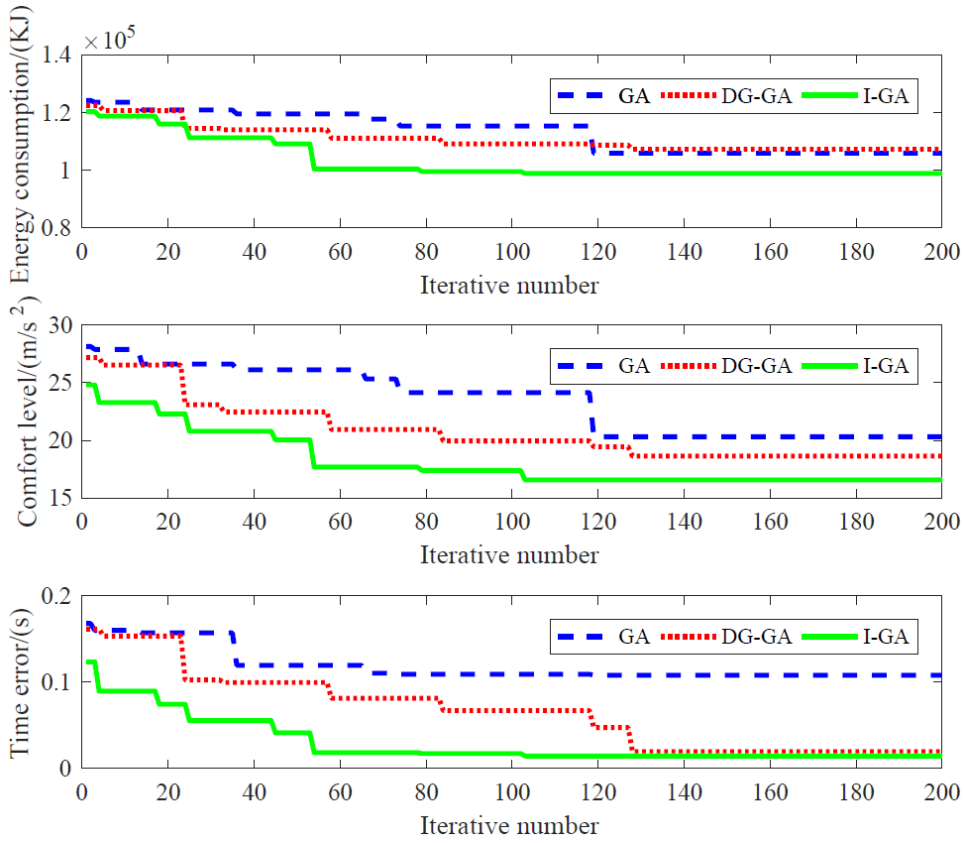

FIGURE 13. Iterative convergence curve of each optimization target of three algorithms

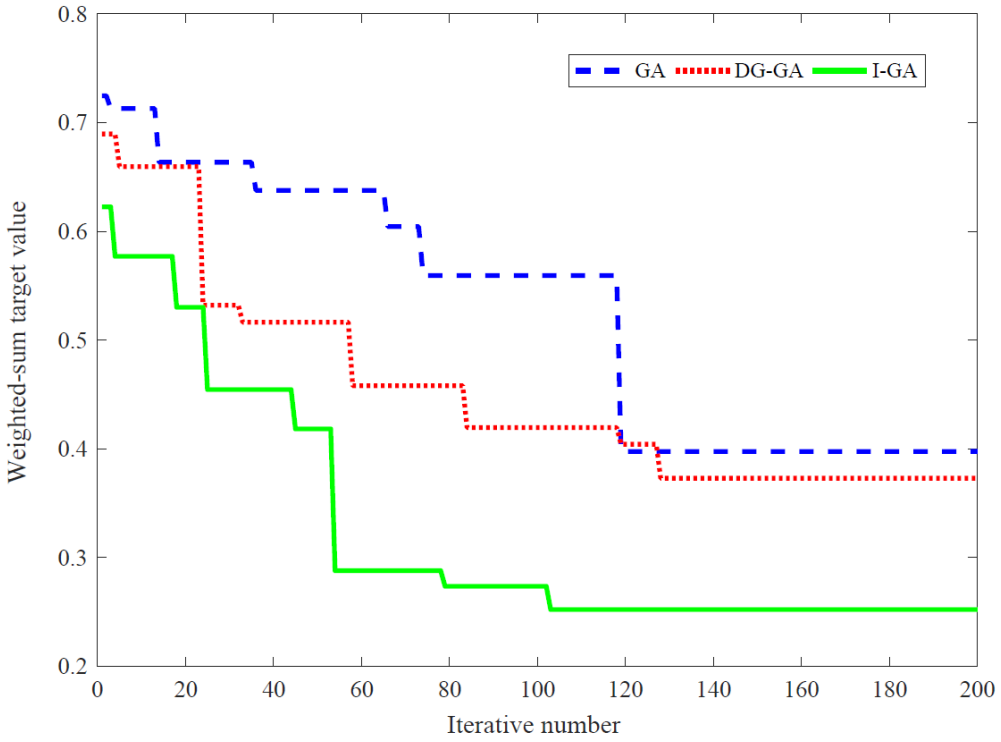

FIGURE 14. The iterative convergence curves of the weighted-sum target value of three algorithms

TABLE 2. Optimization results of three algorithms

Algorithm	Energy consumption	Punctuality	Comfort level	Weighted-sum target
I-GA	98623 KJ	0.0101 s	15.132 m/s^2	0.2603
DG-GA	107213 KJ	0.0154 s	19.178 m/s^2	0.3819
GA	105910 KJ	0.1126 s	20.498 m/s^2	0.4012

11 and Figure 12 that the I-GA can obtain extremely simple control sequence and make the maximum use of the long downhill and uphill section. It can be seen from Figure 13 and Figure 14 that the I-GA has fast convergence speed and strong global optimization ability.

4.4. **HIL simulation results and analysis.** The above MATLAB simulation is a pure simulation technology separated from the actual operation environment of the train. In order to more effectively verify that I-GA has better optimization performance, dSPACE HIL simulation technology is adopted in this paper. Train HIL simulation technology is based on the half-physical environment of the train, and the optimization algorithm and control algorithm are written into the optimizer and controller respectively, so as to get the simulation results close to the real situation. HIL simulation has real on-board equipment, including sensors, optimizer, controller, connector, conditioning circuit, signal processing unit and so on, as shown in Figure 15. In Figure 15, Loop1 is "low-level control behavior loop", and Loop2 is "high-level optimization strategy loop". Loop1 is isolated (the red dotted box in Figure 15) because the main research of this paper is optimization problem. According to HIL simulation platform of Dalian NO.12 light rail line, GA, DG-GA and I-GA are respectively adopted to solve the optimization model of train operation process, and the obtained optimization results are shown in Figure 16 to 18 and Table 3.

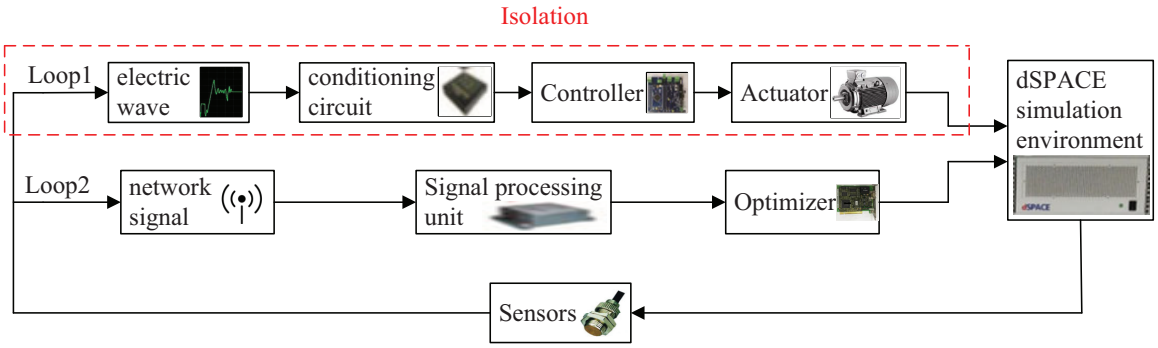

FIGURE 15. HIL simulation structure

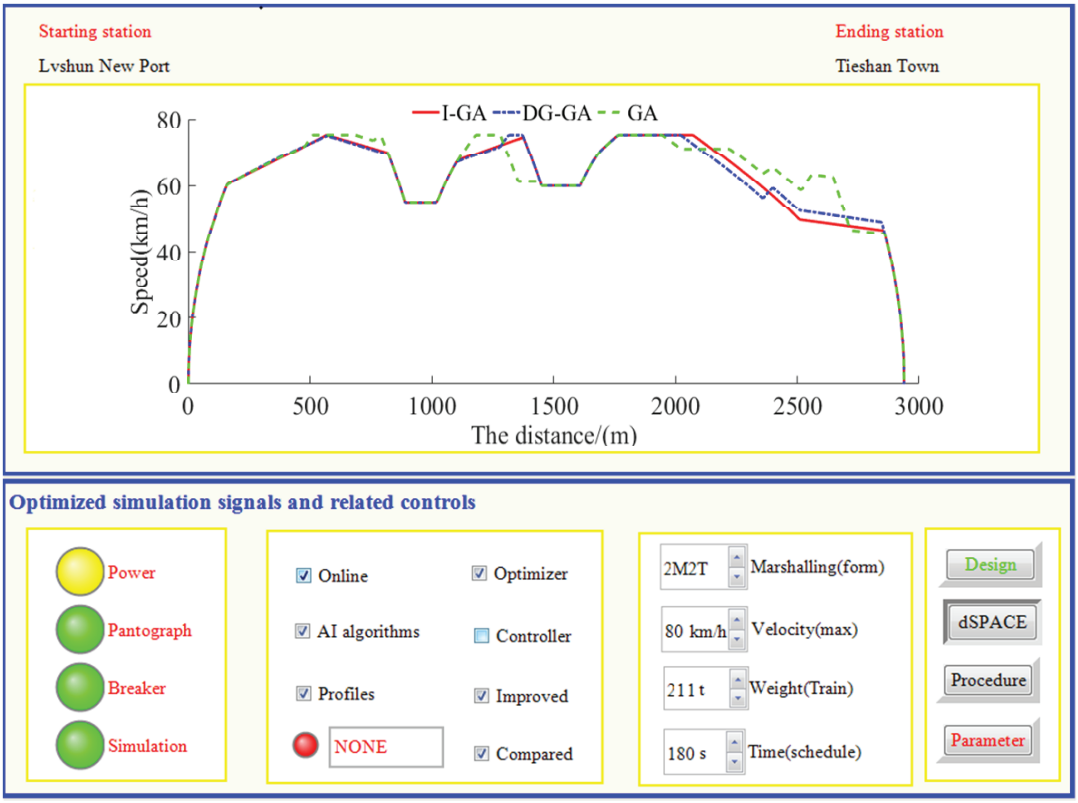

FIGURE 16. The speed distance graph of optimal results

In Figures 16-18, the regional options show HIL is online, the controller is isolated, and the optimizer is in operation. When "Profiles" is selected, the speed distance graph of optimal results is displayed, as shown in Figure 16. When the multi-option button is "(u, s) sequence", the train operation control sequence can be displayed, as shown in Figure 17. When the multi-option button is "iteration PRO", relevant iterative convergence curves can be displayed, as shown in Figure 18.

To further verify the optimal performance of I-GA, the paper also considers the case that the controller is not isolated (the devices of the red dotted box are retained in Figure 15), and the controller adopts predictive control algorithm. The obtained speed distance curve and simulation results are shown in Figure 19 and Table 4. In Figure 19, three black curves are the optimization curves corresponding to the above three algorithms, namely, Ideal Curves (IC). The other three control curves almost coincide with the corresponding

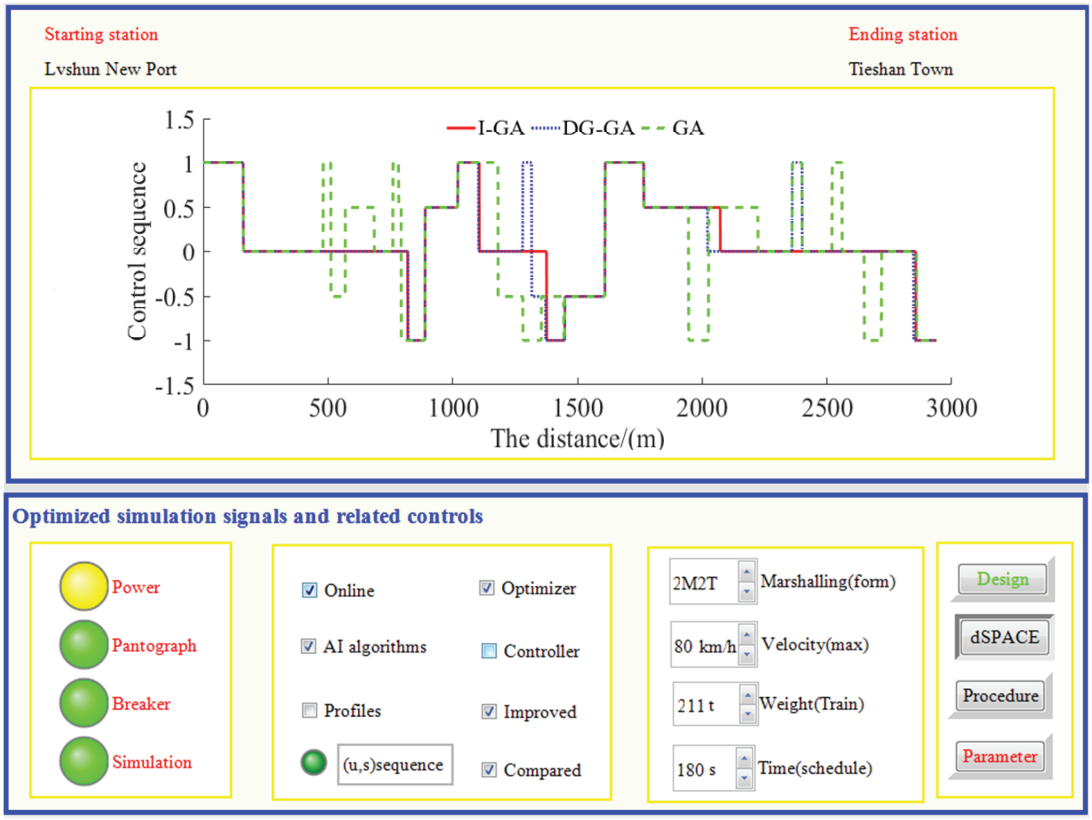

FIGURE 17. Train operation control sequence

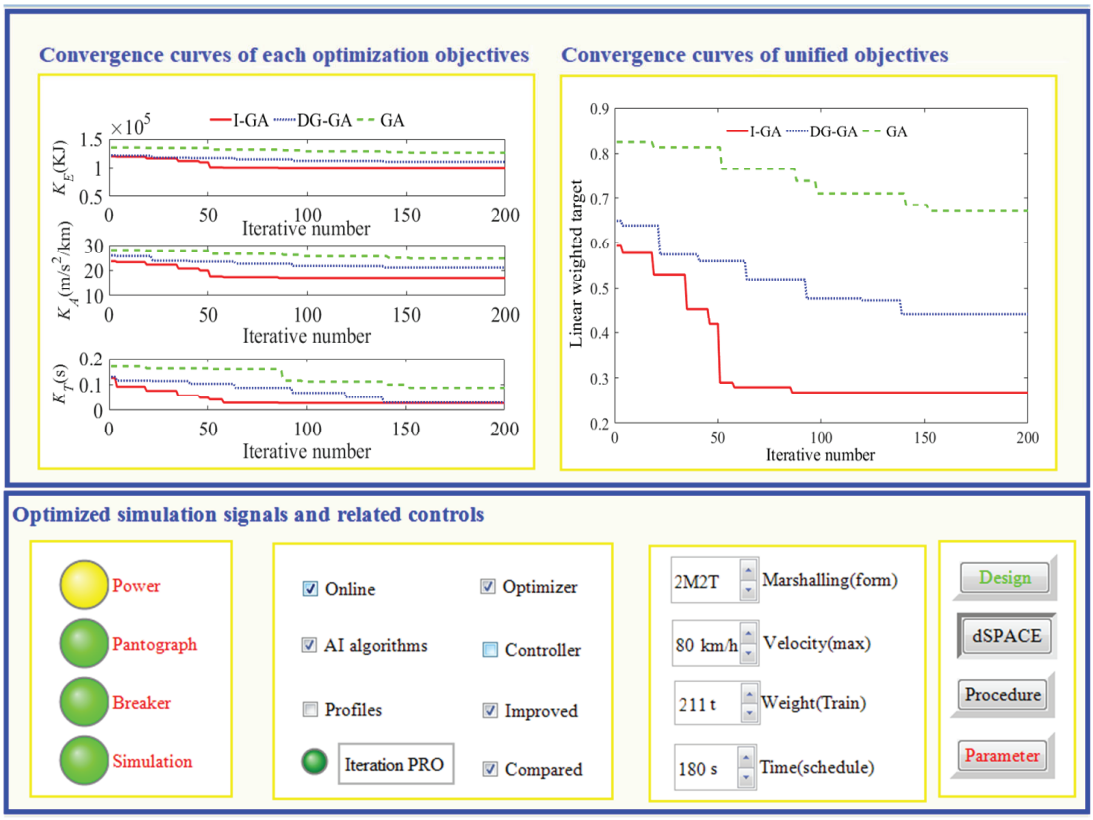

FIGURE 18. The relevant iterative convergence curves

TABLE 3. Optimization results of three algorithms

Algorithm	Energy consumption	Punctuality	Comfort level	Weighted-sum target
I-GA	99332 KJ	0.0263 s	17.081 m/s^2	0.2680
DG-GA	109721 KJ	0.0258 s	21.133 m/s^2	0.4438
GA	119850 KJ	0.0872 s	24.758 m/s^2	0.6704

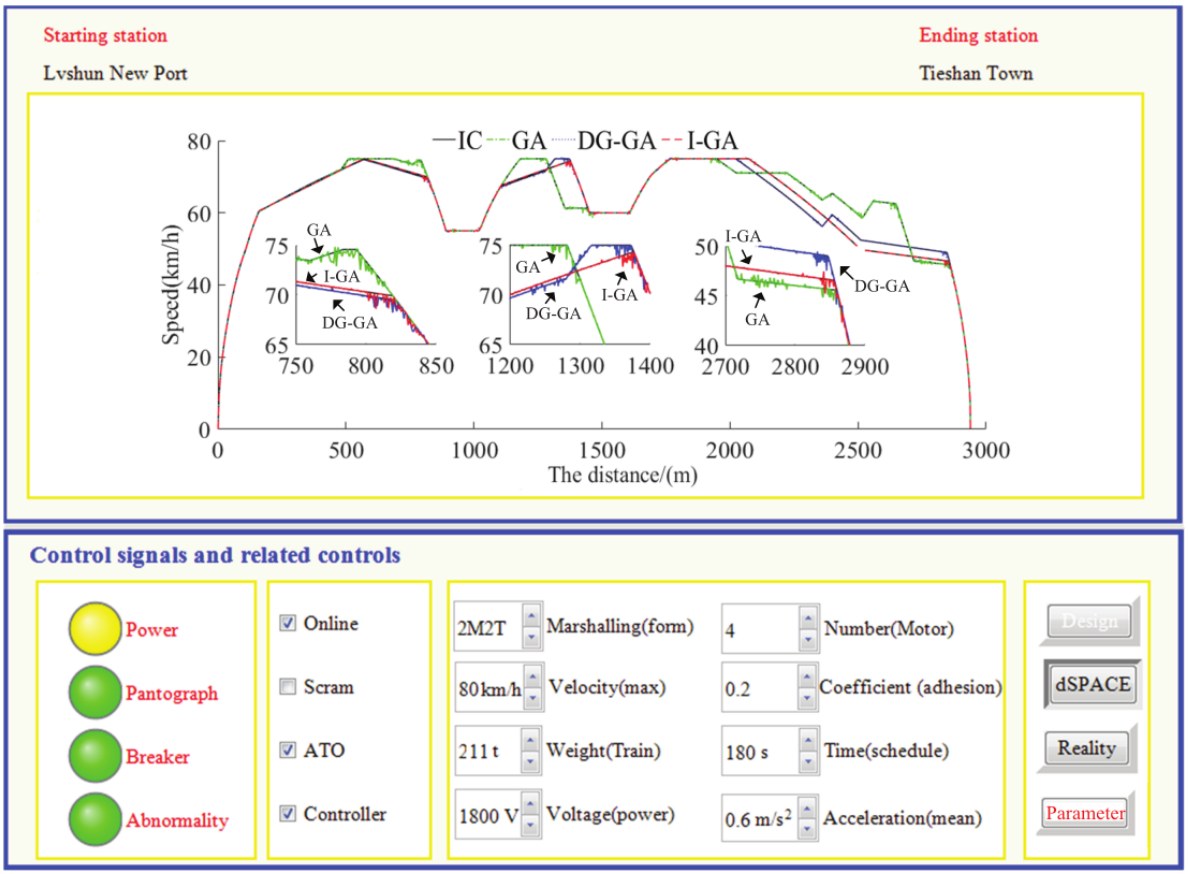

FIGURE 19. The relevant iterative convergence curves

TABLE 4. Optimization results of three algorithms

Algorithm	Energy consumption	Punctuality	Comfort level
I-GA	103582 KJ	0.0415 s	42.956 m/s^2
DG-GA	120595 KJ	0.0597 s	70.190 m/s^2
GA	140470 KJ	0.1148 s	87.218 m/s^2

ideal curves (there are 6 curves in Figure 19). Because of the delay and jitter in the half-physical simulation, all the control curves in the three enlarged areas in Figure 19 have burrs and unsmoothness, which is closer to the actual operation of the train.

As can be seen from the HIL simulation results, HIL simulation and MATLAB simulation have similar optimization results. Compared with GA and DG-GA, the three performance indexes (including energy saving, punctuality and comfort) obtained by I-GA have been greatly improved. Therefore, HIL simulation also proves that I-GA has stronger optimal ability.

5. **Conclusions.** Traditional GA uses random rules to search in the global scope. For complex line conditions, the search speed for feasible solution is slow. Therefore, this paper conducts DM and GM on the related genes according to the type of penalty function term. This method can avoid the blind searching and greatly accelerate the search for feasible solutions. The new adaptive probability formula enables the chromosomes to timely adjust the crossover and mutation probability according to their fitness function values, which can avoid the over-reproduction of good individuals and the premature convergence in the early stage of evolution. GA is prone to local convergence in the late stage of iteration. Compared with the Euclidean distance, the fusion distance can take account of the correlation and independence among variables. So, the fusion distance can be used to detect the existence of individual aggregation phenomenon in this paper, so as to better restrain the local convergence for GA.

In addition, there are three classical operations in GA, and only the mutation operation is improved in this paper. In the future, selection and crossover operations can be further improved to achieve better results.

Acknowledgment. This research is supported by National Natural Science Foundation of China (60574018) and the Inner Mongolia Autonomous Region Natural Science Foundation (2017BS0605).

REFERENCES

[1] H. Moradi and H. Ebrahimpour-Komleh, Development of a multi-objective optimization evolutionary algorithm based on educational systems, *Applied Intelligences*, vol.48, no.9, pp.2954-2966, 2018.

[2] J. Meng, R. Xu, D. Li and X. Chen, Combining the matter-element model with the associated function of performance indices for automatic train operation algorithm, *IEEE Trans. Intelligent Transportation Systems*, vol.20, no.1, pp.253-263, 2019.

[3] N. A. AL-Madi, K. A. Maria, E. A. Maria and M. A. AL-Madi, A structured-population human community based genetic algorithm (HCBGA) in a comparison with both the standard genetic algorithm (SGA) and the cellular genetic algorithm (CGA), *ICIC Express Letters*, vol.12, no.12, pp.1267-1275, 2018.

[4] J. Meng, M. Yin, W. Qi et al., Optimization of tracing target curve of high speed train ATO based on genetic algorithm, *Computer Engineering and Applications*, 2016.

[5] C. Sicre, A. P. Cucala and A. Fernández-Cardador, Real time regulation of efficient driving of high speed trains based on a genetic algorithm and a fuzzy model of manual driving, *Engineering Applications of Artificial Intelligence*, vol.29, pp.79-92, 2014.

[6] G. Wang, S. Xiao, X. Chen and X. Li, Application of genetic algorithm in automatic train operation, *Wireless Personal Communications*, vol.102, no.1, 2018.

[7] H. Shi, Q. Peng and H. Guo, Improved GA of train operation simulation model, *The 1st International Conference on Transportation Engineering*, 2007.

[8] Y. Liang, H. Liu and C. Qian, A modified genetic algorithm for multi-objective optimization on running curve of automatic train operation system using penalty function method, *International Journal of Intelligent Transportation Systems Research*, vol.17, no.1, pp.74-87, 2019.

[9] Y. Huang, X. Ma and S. Su, Optimization of train operation in multiple interstations with multi-population genetic algorithm, *Energies*, vol.8, no.12, pp.14311-14329, 2015.

[10] Y. Cao, L. Ma and Y. Zhang, Application of fuzzy predictive control technology in automatic train operation, *Cluster Computing*, 2018.

[11] P. Howlett, An optimal strategy for the control of a train, *The Journal of the Australian Mathematical Society Series B Applied Mathematics*, vol.31, no.4, pp.454-471, 1990.

[12] G. Liu and X. Wang, Fault diagnosis of diesel engine based on fusion distance calculation, *Advanced Information Management, Communicates, Electronic and Automation Control Conference*, pp.1621-1627, 2017.